Stray Magnetic Field Analysis Applied to the Internal Unbalances of Low Power Single Phase Induction Motor

Vincent Fedida, Laure-Line Rouve, Olivier Chadebec, Lauric Garbuio, Sébastien Lemaitre, Thierry Tollance, L. Weber

Stray Magnetic Field Analysis Applied to the Internal Unbalances Diagnosis of Low Power Single Phase Induction Motor

V. Fedida[1,2], L-L Rouve[2], O Chadebec[2], L. Garbuio[2], S. Lemaitre[1], T. Tollance[1], L. Weber[1]

[1] 50 avenue du Nouveau Monde 74307 Cluses Cedex France Tel 00 33 4 50 96 70 00
[2] G2Elab 21 avenue des martyrs CS 90624 38031 Grenoble CEDEX 1 France Tel. +33 (0)4 76 82 62 99

The aim of this paper is to detail the diagnosis of a low power single phase induction motor with capacitor based on the measurement of the stray magnetic field. However, as the magnetic behavior of the studied machine is quite complex, many unbalances exist together and at significant levels. In order to distinguish them, an analytical study and modeling are carried out. The characterization of each unbalance is done using the traditional frequency analysis but also graphic spatial analysis based on retrieved information from several sensors. As a result, representations of the induction with and without the unbalances are illustrated in various ways.

Index Terms—
Fault monitoring, induction motor, stray magnetic field analysis

I. Introduction

Single phase induction motor is widely used in domestic appliances. It requires a single phase supply, which is easily accessible. Additionally, it has a simple construction, a high reliability, and an overall low cost. All these aspects make it convenient to home use such as fridge, fans, wash machine, roller blind and others. The satisfying machine performance lays on a basic conception. As a consequence, the comportment of the highlighted machine in normal running mode involves some magnetic unbalances, high saturation, and phase unbalance. Furthermore, some mechanical imperfections appear from the industrial process and lead to eccentricity due to the misplacement of axes. All these factors added together make the magnetic behavior complex. Conjointly, the acoustic spectrum is very rich and some mixed unbalances generate disturbing noises that can have electromagnetic origins. In order to predict these troublesome effects and to assess each machine quality, diagnosis is required.

As an electrical machine relies on electric, magnetic and mechanical phenomena, numerous diagnosis methods can be associated to it [1]-[4].

Among them, the stator currents diagnosis is the most used. This provides non invasive technique studied by many authors and led to the identification of some signatures and warning thresholds for each fault [2],[5]-[7]. However, with no load or with inaccurate speed values, this analysis is difficult to handle. Moreover, this method has been not often applied to single phase induction motors [17].

Vibrations analysis is also widely investigated [2], [8]-[10]. This non-invasive method gives information about the electromagnetic local forces distribution in the machine. Various vibrations sources including mechanical elements displacement can also be detected. They can perform a large diagnosis, but are faced to considerable frequency content in our application.

The air-gap induction is a key-element for electrical motors. Nevertheless, its direct measurement is not easy and requires the implementation of a magnetic sensor in the air-gap. An original alternative is the leakage flux measurement. Indeed, its harmonics spectrum is similar to the one which flows in the air-gap but with a reduced module. This non-intrusive method has been under development for the past 10 years [2], [10]-[12] and has already applied to synchronous motors [10] and induction motors [12]. The leakage flux has a low amplitude compared to air-gap flux (µT against T), and its evaluation needs suitable sensors.

In this paper stray field diagnosis is investigated to characterize unbalances. Firstly, unbalanced outcomes on air-gap induction are analytically studied. Secondly, by using numerical simulations, magnetic stray field is compared to air-gap one. After these two steps, we are able to identify and specify a signature for each unbalance. This task is done using spectral and spatial techniques. Finally, the developed technique is applied to different machines.

II. Electrical Machine and Experimental Set-up

A. *Motor Features*

There is some single phase motor design. The main difference deals with starting systems composed by a temporally or permanent auxiliary winding. We focus on a single phase induction motor with permanent capacitor (Fig.1)

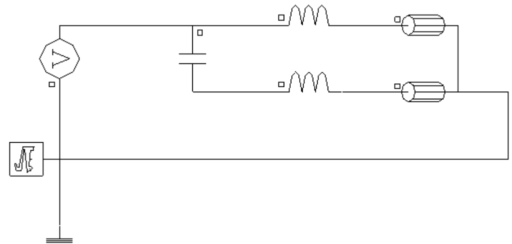

Fig.1 Electrical Diagram of the Motor supply

The actuator characteristics are:

- Torque : 6N.m
- Supply : 230V/50Hz
- Capacitor : 3.3µF (±7%)
- Power : 90W
- 2 poles
- Air-gap : 0.365mm

- 12 stator slots
- 16 rotor bars
- 5/6 Winding

B. Numerical Modeling

For simulations, the finite elements method (FEM) is used with Flux software. Due to the 2D representation, magnitudes of stray field are incorrect, even if spectral frequency content is correct.

Low frequencies events are one challenge of these simulations which requires long running time. Furthermore, with mechanical faults machine, symmetry is not allowed. In addition to airgap region, surrounding air is also finely meshed. So even in cases of 2D simulations, computation times are long. For these simulations, machine runs in no-load mode.

C. Sensors and experimental set-up

In stray flux diagnosis, coils are often used to measure the field [12],[15]. However, in this work, we use fluxgate sensors [18] authorizing the measurements of nT to mT range and on a spectrum from DC to a few kHz. Compared to coils, they have a good precision for low frequencies fields. This sensor technology has already been used in [10] for a stray field diagnosis purpose.

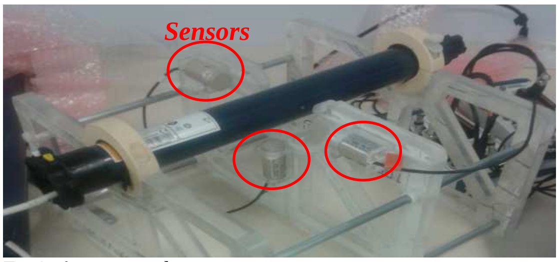

Fig.2 Actuator and sensors

Two sensors positioning are used for stray field measurement. Near to the end-winding with a recover of axial component [12], taking advantage of a machine is typically less armored axially and be more permeable to the field. Another sensor position is in front of the stator and associated to radial component measurement, which has the advantage of being more easily studied in modeling. For these reasons, sensors are put like the second configuration, to recover the radial field of the machine.

Fig.3 illustrates the way of measure, with sensors in the air region and motor produces stray magnetic field. For a first approach, we decide to use three sensors. Each recovers radial, tangential and axial components. Two sensors are positioning on a machine diameter (sensor 1 and sensor 3 in Fig.3), to facilitate the identification of some effects like static eccentricity. A third sensor positioning at 90° helps us to identify the difference of current feeding between the two 90° phases. Distance between our sensors and machine can be changed.

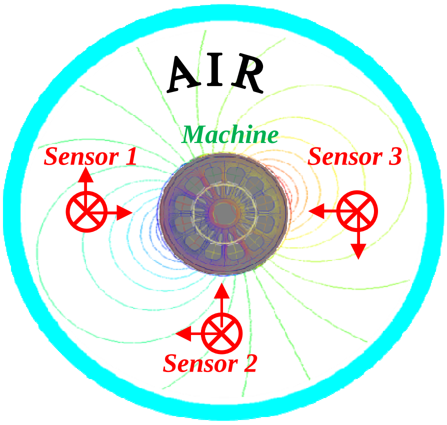

Fig.3 Illustration of measurements method

Each sensor is numbered in order to simplify the comprehension in the following part.

D. Analyze

Some signal processing techniques are used. The first is the classical Fourier transform which allows us to analyze frequency effects. Sampling frequency is chosen at 2 kHz, authorizing us to see effects under 1kHz. This bandwidth contains the principal magnetic effects existing in this machine. Due to its design with several unbalances, frequency spectrum of stray field in simulation seems very complex (Fig.4), furthermore some effects act at same frequency.

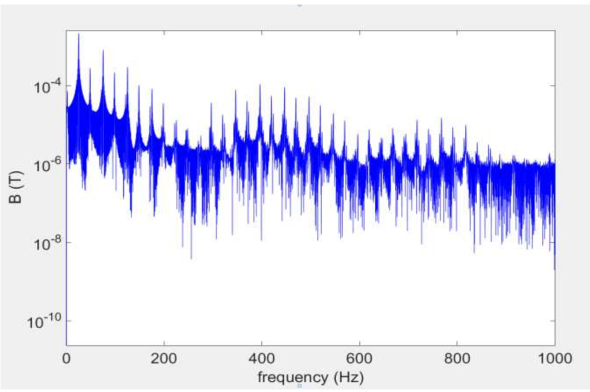

Fig.4 Spectrum of stray field with faults in simulation

The difficulty of Fourier analysis leads us to develop new original representation technique in order to bring more understandable information.

As the machine is long (size / diameter ratio), in its middle the axial field is minimal. Then the measured magnetic field is mostly radial and tangential. By combining these two components in one plane, we are able to plot the direction of magnetic field vector and its magnitude. As a result we get a picture of our rotating field at a point in space. This kind of representation is equivalent to a Lissajou curve (Fig. 5), and permits to see the fields' nature (rotating or pulsating) and their actions.

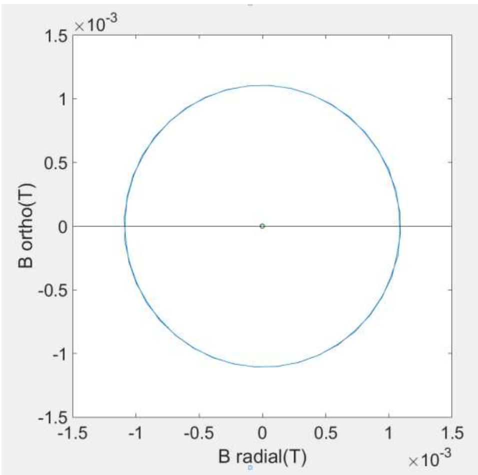

Fig.5 Lissajou of stray rotating field for an equilibrate and unfaulty machine in simulation

In the case of a perfect motor (no fault, no saturation and no unbalance) like Fig. 5, field is purely rotating and describes a circle in the Lissajou curve. With the apparition of unbalances, this circle will be distorted. In the case of faulty motors with saturation, eccentricity and phase unbalance this curve become as shown in Fig.6

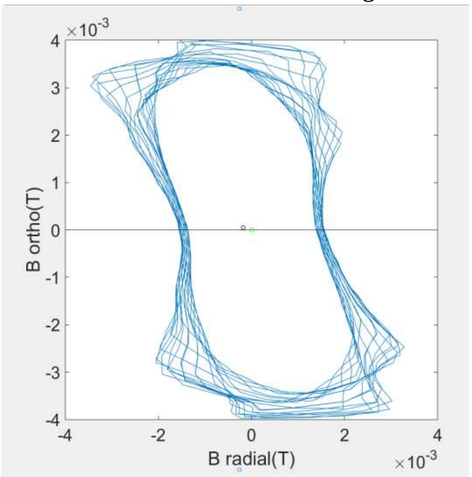

Fig.6 Lissajou of stray rotating field for a unbalanced supply, saturated and faulty machine in simulation

In the following part, we will see step by step how machine unbalances can change Lissajou curve from (Fig. 5) to (Fig.6). This rotating field representation is really intuitive and helps for characterization of unbalances. Some tools will be developed using this curve.

III. Unbalances study

In the studied machine, these unbalances exist generally:

- Unbalanced current
- Static eccentricity
- Dynamic eccentricity
- Saturation

We try to identify them except saturation. This magnetic phenomenon complexes the study, but doesn't advise us on specific harmful behavior in machine. Test-bed allowing low current supply; saturation will be excluding of the study. Slot effects are neglected too.

As stated previously, stray magnetic flux and air-gap induction have the same frequency spectrum. In order to study faults analytically, we purpose to analyze the air-gap induction B.

$B(t,\theta) = p(t,\theta).\varepsilon(t,\theta)$ in Tesla (1)

where

$p(t,\theta). = \dfrac{\mu_0}{g(t,\theta)}$ (2) : Air - gap permeance (Wb.A^{-1})

$g(t,\theta)$: Air - gap (m)

$\varepsilon(t,\theta)$: Magnetomotrices forces acting on airgap

With $\mu 0$ the air permeability

For a machine without any unbalances and considering only the first spatial harmonic, induction can be expressed:

$B(t,\theta) = B_0 \cos(2\pi f_s t - p\theta)$ (3)

Frequency content can be express in this way:

{ $fs; p$ } (4)

where B_0 the amplitude of the rotating induction, fs the supply frequency, p the number of poles pairs.

Equation (4) used in [16], permits to express easily spatial and temporal frequencies of the field. Knowledge of magnetic spatial behavior is necessary for stray field diagnosis. Each sensor located in a specific θ position, some variations take place around the motor and the sensitivity of sensors position related to the considered unbalance is a critical point.

A. *Unbalanced currents*

Electrical unbalance occurs when the currents flowing in the different phases have not the same amplitude, not an ideal phase shift or identical shape. It usually appears from a power failure or a short circuit between turns of a winding. In our case, the auxiliary winding capacitor causes this unbalance. The amplitude, shape and phase of currents are different. Magnetomotive forces (MMF) change. Usually MMF produced by each winding are designed to obtain a global rotating field. In unbalance case, some elements of one phase do not recombine with the second and lead to parasitical pulsating fields.

$B(t,\theta) = B_0 * \cos(wt - p\theta) + \sum_k Bp_k * \cos(wt)\cos(p\theta + \varphi_k)$ (5)

where Bp_k is the pulsating field magnitude, φ_k the phase of a pulsating field, k the number of pulsating fields.

Under pulsating fields influence, machine doesn't become spatially balanced as it can be seen in Fig.7 with same time acquisition in simulation with two different sensors (sensor 1 and 2)

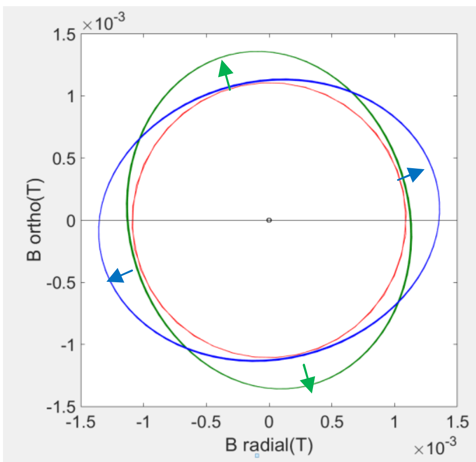

Fig.7 Simulation results of pulsating unbalance field variation with two sensors at 90°(blue sensor 1 and green sensor 2), in red: rotating field of machine without unbalance.

A simple way to analyze this is to observe the spatial variations of rotating field magnitude (Fig. 8).

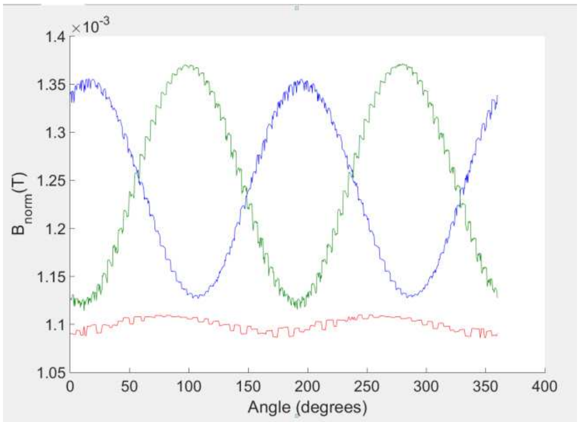

Fig.8 Simulations results of Lissajou magnitude variation for two sensors at 90°(blue sensor 1 and green sensor 2), in red: Lissajou magnitude of machine without unbalance.

Pulsating field existence shine in Fig.8. Spectral analysis enable quantification of unbalances with the apparition of harmonic two corresponding of the time-variation of pulsating field.

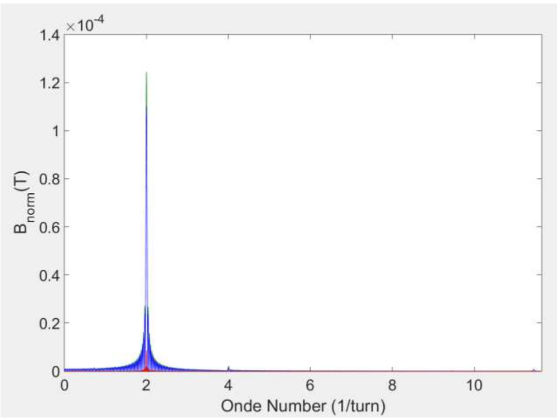

Fig.9 Frequency content of Lissajou magnitude

However this criterion is sensitive to the position of sensor related to the winding and unbalances orientation. Robustness of diagnosis depends on this sensitivity. A future study to consider this sensitiviy and sensors positionning is planned. The ultimate objective is to be free in sensors positionning. For the moment, we need to put them in a favored position.

B. Static eccentricity

Static eccentricity is a mechanical unbalance corresponding to a displacement of the rotor and axis of rotation relative to the stator. Spatial variation of air-gap happens.

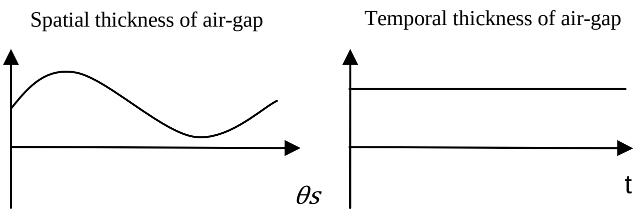

Fig.10 Variation of airgap during static eccentricity

This air-gap variation is:

$$g = g_0 + g_{exc\_stat}\cos(\theta + \varphi_{exc\_stat}) \quad (6)$$

According to (2), permeance changes. [15] has shown that it can be expressed in this way :

$$p(t,\theta) = \frac{\mu_0}{g_0}\left(1 + \frac{g_{exc\_stat}}{g_0}\cos(\theta + \varphi_{exc\_stat})\right) \quad (7)$$

Where g_{exc_stat} is the amplitude of the eccentricity, φ_{exc_stat} is the phase between eccentricity and angular position reference.

Additional frequencies appear:

$\{ f_S ; 2\theta \}$ (8)

$\{ f_S ; 0 \}$ (9)

New frequencies are only spatial one, thus with time frequency decomposition, we cannot provide information. Spatial comportment recognition can detect static eccentricity using differential method. With two magnetic poles, the magnetic behavior of machine is the same on a diameter at mechanical unbalances closely**.** This can be observe on Lissajou curve in simulation (Fig.11)

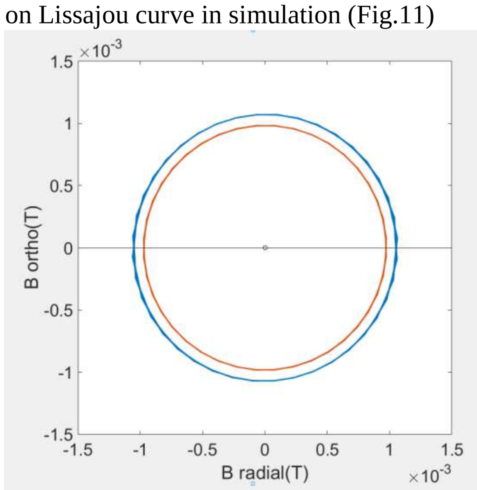

Fig.11 Stray field Lissajou: simulation of static eccentricity(20%) two sensors opposite by a diameter

A simple criterion to identify this phenomenon is to compare the area of the two opposite Lissajou curve. The eccentricity variation is sinusoidal; theoretically the three sensors are able to identify this comportment. In this simulation, sensors are located in the best position to see eccentricity.

C. Dynamic eccentricity

Dynamic eccentricity corresponds to a misplacement of the rotor axis compared at rotation axis. This mechanical unbalance comes out during the actuator assembly. It brings tiredness of different elements and can create specific noises particularly troublesome for users. Airgap modulate, spatially and temporally according to the rotation speed.

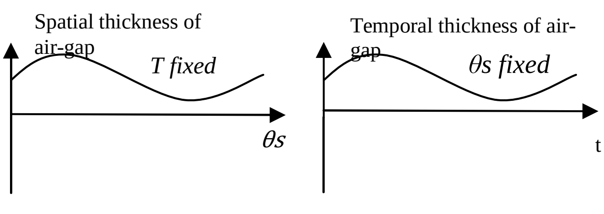

Fig.12 Variation of airgap during dynamic eccentricity

$$g(t,\theta) = g_r + g_{excd} \cos(\omega_r t - \theta + \varphi_{exc\_dyna}) \quad (10)$$

Where g_0 mean of the airgap, g_{excd} amplitude of eccentricity, ω_r speed of rotation, φ_{exc_dyna} phase between eccentricity and angular position reference.

$$p(t,\theta) = \frac{\mu_0}{g_0}(1 - \frac{g_{excd}}{g_0}\cos(\omega_r t - \theta + \varphi_{exc\_dyna})) \quad (11)$$

In permeance equation, eccentricity fault frequency is expressed in this way

$$\{ f_r ; 1 \} \quad (12)$$

We have the relation:

$$f_r = \frac{1-s}{p} f_s \quad (13)$$

with s the slip

When dynamic eccentricity occurs, induction spectrum acquires the following frequencies:

$$\{ \frac{2-s}{p} f_s ; 2\theta \} \quad (14)$$

$$\{ \frac{s}{p} f_s ; 0 \} \quad (15)$$

Additional temporal frequencies appear and can be picked up in spectrum. Knowing that p=1 spectrum is (Fig.13)

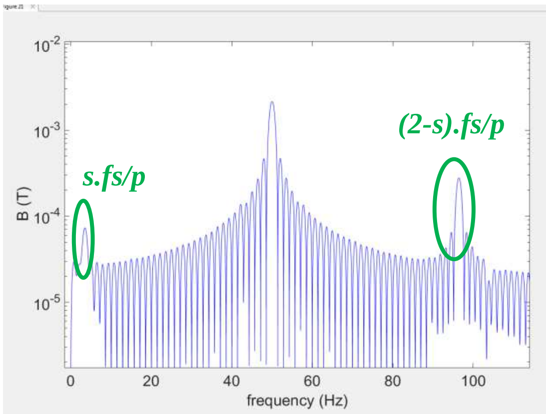

Fig.13 Low frequency in stray field by EFM simulation

Lower frequency has a singular interest in stray field analysis. It takes the advantage of being few attenuated by eddy currents; furthermore low-energy frequencies range is almost empty facilitating its measurement. Finally, this frequency carries the slip information. With its measurement, average rotation speed is known.

According to (10) modulating air-gap acts as a modulation of induction at rotation speed. This can be observe by Lissajou analysis, with the thickness of the curve (Fig.14)

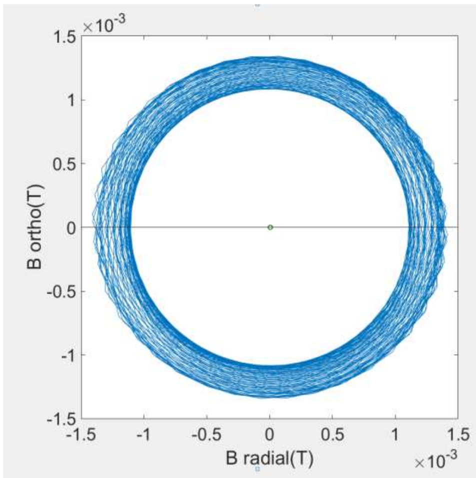

Fig.14 Stray field Lissajou: simulation of dynamic eccentricity (30%)

The thickness informs us about the eccentricity gravity. Note that the outer and inside contour of the curve correspond to fault-free representation with a minimum and maximum air gap.

IV. Measurements and Results

Measurement conditions are similarly as Fig.2. Sensors are located at 8cm from the machine housing. Record time is 5seconds. As we have seen previously, spatial position of sensor is important. In these measurements, they are settled in the most favorable position for each unbalance identification.

A. Unbalanced current

In order to clearly see pulsating field, sensors are put in front of windings. Compared to FEM simulation, a problem appears in Lissajou plotting. In numerical results, radial and tangential stray field are compute in the same element. But in reality, there are a physical separation between tangential recover part and radial recover part of the sensor. This difference deforms Lissajou curve and can attenuated some effects. A solution to palliate this is to use radial component in sensor 1 or 3 and radial component in sensor 2. We obtain the same axis as a radial/tangential measurement, but with an amplified magnitude. Fig.15 showing pulsating fields actions. Nevertheless, this method downside is mechanical unbalances act otherwise, but nonetheless they have a smaller action on the field compared to magnetic unbalances. Signature can be extract. To test criterion, a machine is supplied by three increasingly serious unbalances (amplitude and phase shifting) to simulate capacitor influence (Fig.15)

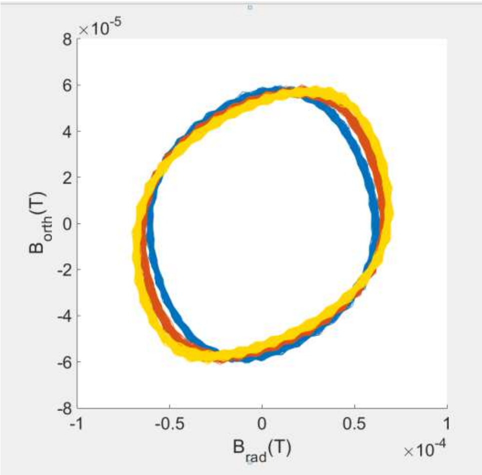

Fig.15 Lissajou curve 95° 50/55V supply (blue), 100°50/60V supply(orange) and 105° 50/65V supply (yellow)

Lissajou deformation distinctly appears. Harmonic two of this magnitude variation is exposed Fig.16

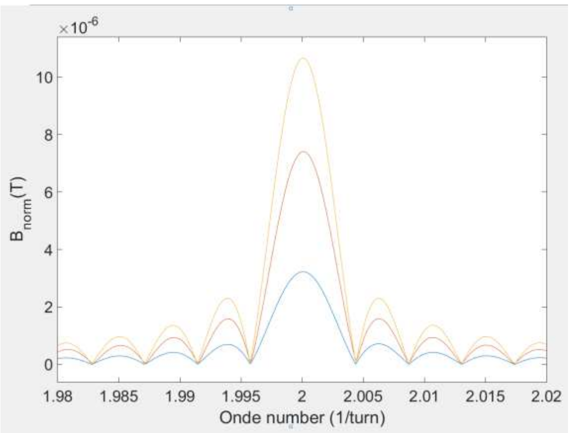

Fig. 16 Harmonic 2 of Lissajou curve magnitude 95° 50/55V supply (blue), 100°50/60V supply(orange) and 105° 50/65V supply (yellow)

This criterion is very sensitive, and can detect unbalance weight. In a second time it can be linked to a capacitor value.

B. Static eccentricity

Mechanical unbalances are more problematic to study experimentally. Indeed, in studied machines, this phenomenon can't be control. The real eccentricity level motor is unknown. For measurement, criterion is tested on different motor with balance supply. After finding maximal eccentricity position, field is picked up on the diametrical sensors (1 and 3). Radial/tangential Lissajou are now considered, even if some effects can be attenuated. To improve method and remove dynamic eccentricity effects (thickness of Lissajou), Lissajou areas are computed on average of external and internal contour (Fig.17)

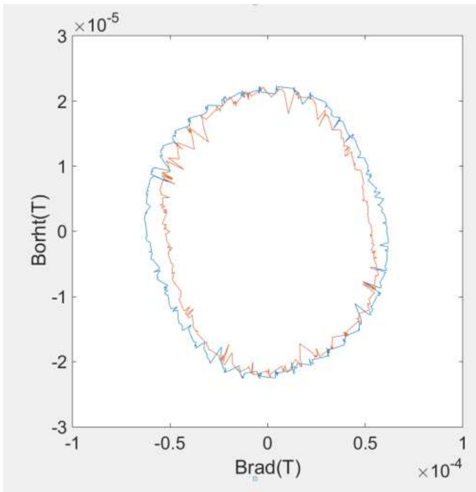

Fig.17 Contour of Lissajou curve for two diametrical sensors

Area difference can be compute for different motor

TABLE I
STATIC ECCENTRICITY ANALYSIS FOR THREE DIFFERENT MOTORS

Motor	Area1/Area2
Motor1	0.86
Motor2	0.89
Motor3	0.94

C. Dynamic eccentricity

In low frequency spectrum, dynamic eccentricity is perfectly perceptible Fig.18.

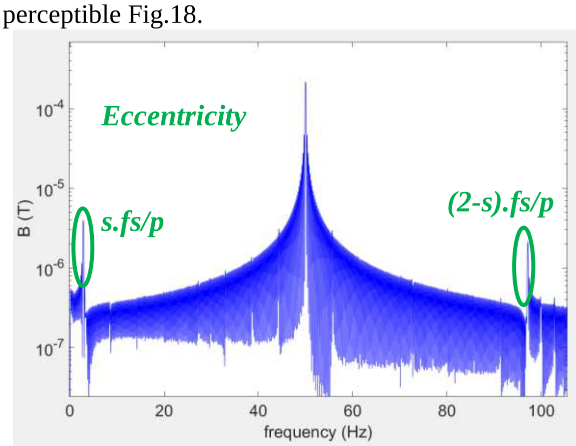

Fig.18 Frequency Stray field content: Low frequencies

Comparison between the three previous motors can be realized Fig.19

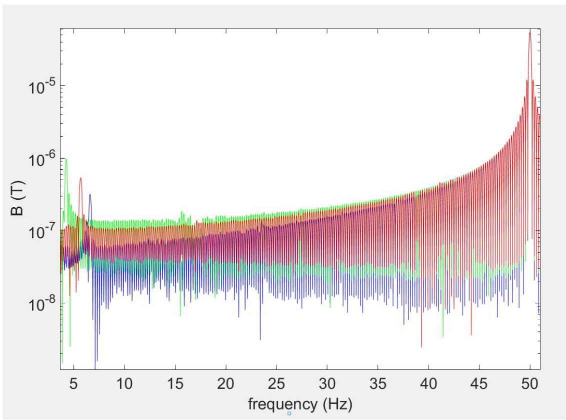

Fig.19 Dynamic eccentricity typical frequency for three different motors

Discrimination between these motors can be provided.
In order to reduce spatial variation due to static eccentricity, eccentricity frequencies can be divided by fundamental. Normalized results are significant in diagnosis process. Currently, this step is not yet established.

V. CONCLUSION

Through this study, a stray magnetic field diagnosis method has been applied to low power single phase induction motors. Several types of unbalances in the machine have been studied analytically and by modeling. For each, a specific signature has been extracted in aim to inform us about the unbalance range. Lissajou curve allows a better visualization and comprehension of magnetic effects. Then different signatures are confronted to real motors. Despite the problem complexity it was possible to collect these signatures and to know a machine state. However some aspects must be improved. This is the case of spatial sensitivity of unbalances. Currently to detect those privileged positions are needed.

VI. REFERENCES

[1] S. Nandi, A. Toliyat, X. Li "Condition Monitoring and Fault Diagnosis of Electrical motors-A Review" *IEEE Trans. On Energy Conversion*,vol.20 n°4 pp719-29 , December 2005

[2] A. Bellini, C.Concari, G.Franceschini,C. Tassoni,A. Toscani "Vibrations,currents and stray flux signals to asses induction motor rotor conditions" *IEE Industrial Electronics IECON 2006* p4963-4968 2006

[3] M. Riera-Guasp,J.A. Antonio-Daviu and G-A Capolino "Advances in Electrical Machine, Power Electronic an Drive Condition Monitoring and Fault Detection : State of the Art" *IEEE Trans. On Industrial Electronics*, vol.62 n°3 pp 1746-1759, march 2015

[4] A. Bellini, F. Filippetti, C. Tassoni and G-A Capolino "Advances in Diagnostic Techniques for Induction Machines" *IEEE Trans. On Industrial Electronics*, vol. 55 n°12 pp 4109-4126, December 2008

[5] J-H Jung, J-J Lee and B-H Kwon "Online Diagnosis of Induction Motors Using MCSA" *IEEE Trans. On Industrial Electronics*, vol. 53 n°6 pp1842-1852 December 2006

[6] W. T. Thomson and M. Fenger "Current Signature Analysis to Detect Induction Motor Faults" *IEEE Industry Applications Magazine* July/August 2001 pp 26-34

[7] H.Henao, H. Razik and G-A Capolini, "Analytical approach of the Stator Current Frequency Harmonics Computation for Detection of Induction Machine Rotor Faults" *IEEE Trans. On Industrial Applications*, vol.41 n°3 pp 801-807 May/June 2005

[8] S.P. Verma, A. Balan "Determination of Radial Forces in Relation to Noise and Vibration Problems of Squirrel-Cage Induction Motors" *IEEE Trans. On Energy Conversion* vol. 9 n°2 p404-412 June 1994

[9] M. Tsypkin "Induction Motor Condition Monotoring: Analysis Technique – a Pratical Implementation" *Electric Machines & Drives Conference (IEMDC), 2011 IEEE International* pp406-411 2011

[10] O. Chadebec,V-P Bui,P. Granjon, L-L. Rouve, N. Le Bihan, J-L Coulomb "Rotor Fault Detection of Electrical Machine by Low Frequency Magnetic Stray Field Analysis" *Diagnostics for Electric Machines, Power Electronics and Drives, 2005. SDEMPED. 5th IEEE International Symposium* 2005

[11] H. Henao, G-A Capolino, C. Martis "On Stray Flux Analysis for the Detection of the Three-Phase Induction Machine Faults" *Industry Applications Conference, 2003. 38th IAS Annual Meeting.* vol.2 pp1368-1373 2003

[12] A. Ceban, R. Pusca, R. Romary "Study of Rotor Faults in Induction Motors Using External magnetic Field Analysis" *IEEE Trans. On Industrial Electronics*, vol. 59 n°5 pp2082-2093 May 2005

[13] S. Tumanski "Induction Coil Sensor- A Review"

[14] O-M. Kwon, C. Surussavadee,V.K. Chari, S; Salon and K. Sivasubramaniam "Analysis of the Far Field of Permanent-Magnet Motors and Effects of geometric Asymmetries and Unbalnce in Magnet design" *IEEE Trans. On Magnetics*, vol. 40 n°2 pp435-442 March 2004

[15] V. Hamata, B. Heller "Harmonic field in induction machines". *Elsevier Scientific Pub. Co*., 1977

[16] J. Lebesnerais "Reduction of Magnetic Noise in PWM-supplied Induction machines Low Noise design Rules and Multi-Objective Optimisation" *Thesis of Laboratoire d'Electricit´e et d'Electronique de Puissance de Lille Ecole Centrale de Lille* 2008

[17] S. Nandi, H-A Toliyat, A-g Parlos "Perfomance Analysis of a Single Phase Induction Motor Under Eccentric Conditions" *IEEE Industry Applications Society Annual Meeting* New Orleans, Louisiana, October5-9 1997

[18] J. Lenz and A-S. Edelstein "Magnetic Sensors and Their Applications" *IEEE Sensors Journal*,vol. 6 n°3 pp 631-649, June 2006